RUSSIAN CHEMICAL REVIEWS
Uspekhi Khimii

April 1972

U.D.C. 541.6 : 541.27

Determination of the Effective Charges of Anions in Media of the Ionic Type by the Positron Method

G.M.Bartenev, A.Z.Varisov, V.I.Gol'danskii, E.P.Prokop'ev, and A.D.Tsyganov

The essential features of the positron method for determining the effective charges of anions in ionic solids are presented, and papers dealing with its application are reviewed. Values of the charges of the anions are given for more than 100 compounds (alkali metal halides, oxides, etc.). In contrast to earlier work, the effective charges of the anions given in this review were determined independently of other methods. Various regular features of the behaviour of the charges in the compounds studied are noted. The bibliography contains 67 references.

The experimental and theoretical study of the annihilation of positrons with the electrons of a substance has revealed a number of possible applications of the effects associated with the annihilation in the study of electronic states in solids[1-5]. Examples illustrating the fruitful nature of the application of the positron-annihilation method include the determination of the energy and topology of the Fermi surface in metals and alloys, the detection of the change in the momentum distribution of electrons in metals and alloys in their plastic deformation, the study of the magnetic structure of ferromagnetic materials, etc. In ionic media, the positron-annihilation method can be used successfully to study the nature of chemical bonds and in particular to determine the effective charges on atoms, produced on the formation of a particular compound. In this respect the positron method may provide a valuable supplement to existing methods such as Szigeti's method, the X-ray spectral method, etc. The present paper presents the essential features of the positron method for the determination of the effective charges of anions in media of the ionic type, based on the "optical" positron model of Gol'danskii and Prokop'ev[6]. To illustrate the method, the values of the charges of the anions are given for more than 100 compounds.

To determine the effective charges of the anions it is possible to use either of two fundamental characteristics of the annihilation: the angular distribution of the annihilation quanta or the lifetimes of the positrons with respect to annihilation.

The annihilation of positrons with the electrons of a substance is most commonly accompanied by the emission of two gamma-quanta at an angle of 180° to one another (in the system of the centre of gravity of the annihilating pair). If the centre of gravity of the pair is moving relative to the observer at a velocity v, the angle between the direction of movement of the photons decreases by an amount of the order of v/c, where c is the velocity of light. The experimental assembly (Fig. 1) is used to determine the deviation from 180° of the angle of separation of the photons (the angle θ). The annihilation quanta are recorded by means of two detectors including NaI(Tl) scintillation crystals with photomultipliers, the signals from which are transferred to a coincidence circuit. Between the detector and the specimen containing the source (^{22}Na or ^{64}Cu isotopes), on each side, there are placed lead screens with narrow slits, one of which—screen 1—is fixed rigidly to the movable detector. The distribution of the pairs of gamma-quanta with respect to θ is studied by measuring the count rate of coincidences in the signals from the detectors as a function of the angle of rotation of one of the detectors relative to the specimen. Since this distribution in fact lies within a small range of

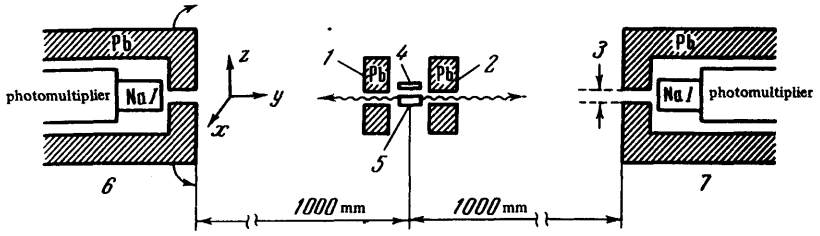


Figure 1. Typical assembly with parallel-slit geometry for the observation of the angular correlation of annihilation quanta: *1*) and *2*) screens; *3*) 1 mm slit; *4*) positron source; *5*) specimen; *6*) moveable detector; *7*) fixed detector.

angles (usually $\theta \lesssim 20$ mrad), it may be assumed that a pair of gamma-quanta moving apart at an angle $(\pi - \theta)$ has a projected momentum on the z axis (see Fig. 1) equal to $p_z = m_0 c\theta$ (m_0 is the rest mass of the electron). The typical form of the $I(\theta)$ curves giving the angular distribution of the annihilation quanta is shown in Fig. 2.

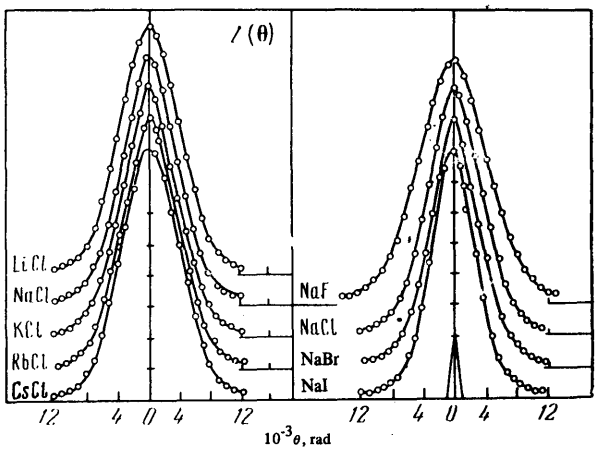


Figure 2. Curves giving the angular correlation of annihilation quanta in alkali metal halide crystals[8].

Observation of the angular correlation of the annihilation quanta gives direct information on the momentum distribution of the annihilating pairs (or electrons, if the movement of the positron can be neglected) in the substance. This is possible since the experimentally observed count rate for the coincidences of the gamma-quanta $I(\theta)$ is related to the momentum distribution density function† $\rho(p)$ for the centres of inertia of the annihilating pairs by the expression[7,8]:

$$I(\theta) = I\left(\frac{p_z}{m_0 c}\right) = \text{const} \int_{p_z}^{\infty} p\rho(p)\,dp; \quad \rho(p) \propto -\frac{1}{\theta}\frac{dI}{d\theta}. \qquad (1)$$

† The momentum distribution $N(p) = 4\pi p^2 \rho(p)$ is often considered instead of the function $\rho(p)$.

Information on the mechanisms of the interaction of a positron with the surrounding electron medium can also be obtained by measuring the lifetimes of the positrons in the substance with respect to annihilation. The lifetime is determined using an assembly (Fig. 3) including a delayed-coincidence circuit. The container with the substance being studied, surrounding the positron source—the ^{22}Na isotope—is placed between two detectors. The moment of generation of the positron is detected by recording the gamma-quantum (detector 1) with energy 1.28 MeV, the emission of which accompanies the β^+-decay of the ^{22}Na nuclei. The moment of annihilation is determined from the production of annihilation quanta with energy 0.511 MeV (detector 2). Fig. 4 gives a typical spectrum of the lifetime distribution of positrons with respect to annihilation in alkali halide crystals. The presence of several decay components with different average lifetimes in the annihilation time spectrum indicates that the mechanism of the annihilation of positrons in ionic crystals is complex. The average lifetimes of the relatively long-lived components are determined from the slope of the plot of the logarithm of the coincidence count rate against the delay time at long delay times.

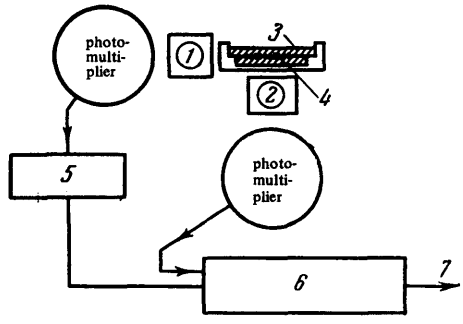


Figure 3. Basic scheme of an assembly for measuring the lifetimes of positrons in condensed media[1]: *1*) and *2*) stilbene crystals; *3*) specimen; *4*) positron source; *5*) delay line; *6*) ~ 10^{-9} s coincidence circuit; *7*) output.

A fairly large number of papers have now been published on the study of the angular distribution of the annihilation quanta and the lifetime distribution of the positrons

with respect to annihilation in different ionic media; halides, oxides, sulphides, and other metal compounds (see, for example, Refs. 1–3 and 8–26). Analysis of experimental results on the study of the annihilation of positrons in ionic crystals shows that the annihilation is preceded by the formation of combined states of the positron, the chief of which are quasi-atomic formations of the e^+–anion type and states of the positronium type (positronium formation is detected from the appearance of a narrow component in the correlation curves and long-lived components in the annihilation time spectra with decay times of the order of 10^{-9} s or more). It has also been noted that if positronium formation is not forbidden energetically, its probability is usually greatly increased by the presence in the medium of defects; of pores (gel), vacancies (irradiated crystals), regions of lower density (glass), etc. Here we shall be interested only in compounds of the e^+–anion type. The formation of these compounds in ionic crystals is preceded by the thermalisation of the positrons, that is their deceleration to thermal velocities. The thermalisation of positrons in ionic crystals is brought about as a consequence of ionisation energy losses, the excitation of electrons into the conduction zone, and by interaction with longitudinal optical phonons. Estimates[27,28] have shown that as a result of all these processes, the positrons are decelerated to thermal velocities in times of the order of 10^{-12} s. Since the shortest lifetime of positrons with respect to annihilation in ionic crystals amounts to several 10^{-10} s,[1,9,22–24,26] it may be assumed that almost all the positrons are able to undergo thermalisation before annihilation. Some of the positrons naturally enter the target and annihilate in flight, that is in the thermalisation process, but experimental results[29–32] and theoretical estimates[27] show that the proportion amounts to only 1–3%.

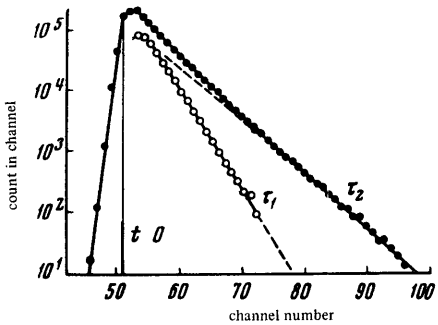


Figure 4. Positron lifetime distribution with respect to annihilation in lithium chloride[9] (one channel = 0.88×10^{-10} s, $\tau_1 = 2.36 \times 10^{-10}$ s, $\tau_2 = 4.35 \times 10^{-10}$ s).

The thermalised positron annihilates in the free state or is captured beforehand by the nearest negative ion. The probability of annihilation of free positrons in media of the ionic type is negligibly small compared with the probabilities of the two-photon annihilation of combined positrons[33]. Thus the annihilation characteristics of ionic crystals in the absence of appreciable positronium yield will be determined chiefly by the properties of the e^+–anion system.

Negative ions (F^-, Cl^-, Br^-, I^-, O^{2-}, S^{2-}, Se^{2-}, and Te^{2-}) have filled electron levels with the structure of inert gas atoms. The positron moves in the field of the nucleus and the electrons of the anion. In this instance we are dealing with a many-electron problem. If however we neglect the deforming action of the positron on the electron levels of the ion, we can regard the movement of the positron in the e^+–anion system as movement in a field of central forces; this is analogous to the model of the optical electron in alkali metal atoms. The "optical" positron model was first proposed by Gol'danskii and Prokop'ev[6]. In this model it is assumed that the positron moves in the Coulombic field of the anion, of the type $U(r) = -\eta e/r$, where $(-\eta e)$ is the effective charge of the anion in the crystal. Since the inner levels of the anion are not accessible to the positron as a consequence of the strong Coulombic repulsion by the nucleus, the wave function of the ground state of the positron in the e^+–anion quasi-atom has been given in the form[6] $r \cdot \exp(-\alpha r)$, where α is a variable parameter. For a combined positron, the correlation of the annihilation radiation is determined by the relative probability[34]:

$$P(k_z) = \frac{\int_{k_z}^{\infty}\int_0^{2\pi} \omega(k)\, k dk d\theta}{\int_0^{\infty}\int_0^{2\pi} \omega(k)\, k dk d\theta}, \qquad (2)$$

where $\omega(k)$ is the probability of annihilation, with the emission of two gamma-quanta with a total momentum $p = nk$, averaged with respect to the spins of the initial states of the electrons and the positron and summed over the polarisations of the radiated photons:

$$\omega(k) = \pi r_0^2 c \sum_{i=1}^{m} \left[h^{-\frac{3}{2}} \int e^{-ikr} \varphi_i(r)\, \chi(r)\, dr\right]^2. \qquad (3)$$

Here, r_0 is the classical radius of the electron, and $\varphi_i(r)$ and $\chi(r)$ the one-electron and positron wave functions respectively for the compound of the e^+–anion type. The summation in Eqn. (3) is carried out over all electrons involved in the annihilation.

The lifetime of a combined positron can be calculated from the equation[35]

$$\tau = 5 \cdot 10^{-10} \frac{\rho_0}{\rho}, \text{ s}, \qquad (4a)$$

where $\rho_0 = (8\pi a_0)^{-1}$ is the electron density at the positronium atom, averaged with respect to the spin states of the electron and positron, and

$$\rho = K \cdot \sum_{i=1}^{m} \int \varphi_i^2(r)\, \chi^2(r)\, dr. \qquad (4b)$$

Here, K is a factor which takes account of the change in the wave functions of the electrons not involved in the annihilation; to a good approximation, it may be assumed that $K = 1$.[33,36]

If we choose Slater exponents as the wave functions of the electrons of the anion, we can use Eqns. (2)–(4) to establish in analytical form the relationship between the chief characteristics of the annihilation of the positron with the electrons of the anion‡ and the effective charge of the anion in the crystal. Within the framework of the "optical" model of the positron, this relationship has the

‡ Usually, only the annihilation of positrons with the electrons of the outer ns^2, p^6-levels of the anions is considered.

following form[6]: the angular correlation of the annihilation quanta for the annihilation of a positron with an *nl* electron of an anion is

$$P_{nl}(k_z) = \frac{\int_{k_z}^{\infty} S_{nl}^2 k^{2l+1} dk}{\int_0^{\infty} S_{nl}^2 k^{2l+1} dk}, \quad (5)$$

where

$$S_{nl} = k^{-l} \int_0^{\infty} r^{n^*+2} e^{-(\alpha+\beta)r} j_l(kr)\, dr, \quad (6)$$

and $j_e(kr)$ represents the spherical Bessel functions (the form of various functions S_{nl} and P_{nl} has been published[6]); the half-width of the correlation curves (the total width at half the height of the curve $P_{ns,p} = 0.25\, P_{ns} + 0.75\, P_{np}$) is

$$\Gamma_{ns,p} = C^{\Gamma}_{ns,p}(\alpha + \beta), \text{ mrad} \quad (7)$$

and, finally, the lifetime of the positron (with allowance for the factor 4π omitted in Ref. 6) is

$$\tau_{ns,p} = 2{,}5 \cdot 10^{-10}\, C^{\tau}_{ns,p}\, \frac{(\alpha+\beta)^{2n^*+3}}{\alpha^5 \cdot \beta^{2n^*+1}}. \quad (8)$$

The following symbols are used in Eqns. (5)–(8): $\alpha = 3/2\eta$, $\beta = Z - \sigma/n^*$ is the Slater exponent (Z is the charge of the nucleus, σ is the screening number, and n^* is the effective principal quantum number), and $C^{\Gamma}_{ns,p}$ and $C^{\tau}_{ns,p}$ are constants, the values of which are determined entirely by the quantum number n. The calculated values of the constants $C^{\Gamma}_{ns,p}$ and $C^{\tau}_{ns,p}$ are given in Table 1.

Table 1. Calculated values of the coefficients $C^{\Gamma}_{ns,p}$ and $C^{\tau}_{ns,p}$ in Eqns. (7) and (8)*.

n	2	3	4	5
n^*	2	3	3.7	4
$C^{\Gamma}_{ns,p}$	3.52	2.86	2.59	2.48
$C^{\tau}_{ns,p}$	$\frac{1}{80}$	$\frac{3}{448}$	$\frac{1}{215}$	$\frac{1}{240}$

* The values of the constant $C^{\tau}_{ns,p}$ for $n = 2$, 3, and 5 were taken from Ref. 6.

The form of the theoretical curves for the angular correlation of the annihilation quanta and the nature of the dependence of the lifetimes of the positrons on the magnitude of the effective charge of the anion are shown in Figs. 5 and 6. The decrease in the half-width of the correlation curves and the increase in the lifetime of the positrons with increase in the number n, that is the principal quantum number of the outermost level of the anions, following from the "optical" model of the positron, and also numerical estimates of these characteristics of the annihilation, show good agreement with results of the measurement of the angular distribution of the annihilation quanta[8] and the lifetimes of the positrons[9] in alkali metal halide crystals.

The direct comparison of the theoretical and experimental curves giving the angular correlation of the annihilation quanta is of interest. The result of this comparison for the oxides of the alkaline earth metals is shown in Fig. 7.

Because of the appreciable scatter in the published values of the charges of the oxygen ion in oxides, the theoretical curves in Fig. 7 were calculated in such a way that their half-width was equal to the half-width of the experimental $I(\theta)$ curves. Comparison of the theoretical and experimental correlation curves is also necessary for the detection of the possible presence, on the curves, of a narrow component due to the annihilation decay of parapositronium atoms. When parapositronium atoms are formed, the calculated and experimental $I(\theta)$ curves do not coincide (see, for example, Fig. 8).

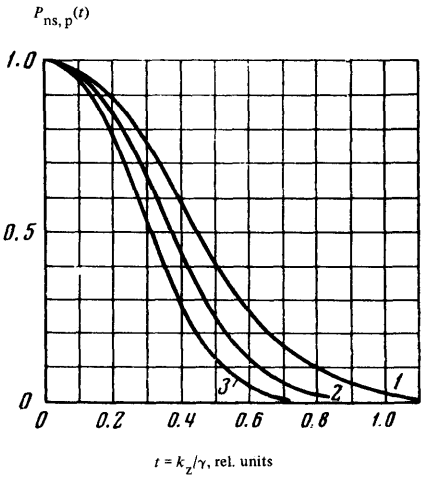


Figure 5. Theoretical angular correlation curves for annihilation quanta: *1*) $P_{2s,p}(k_z/\gamma)$, *2*) $P_{3s,p}(k_z/\gamma)$, *3*) $F_{5s,p}(k_z/\gamma)$, where $\gamma = \alpha + \beta$.

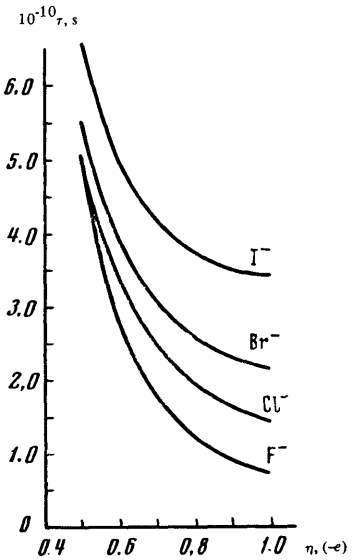


Figure 6. Dependence of the lifetimes of the positrons on the effective charge of the anion η in the "optical" positron model.

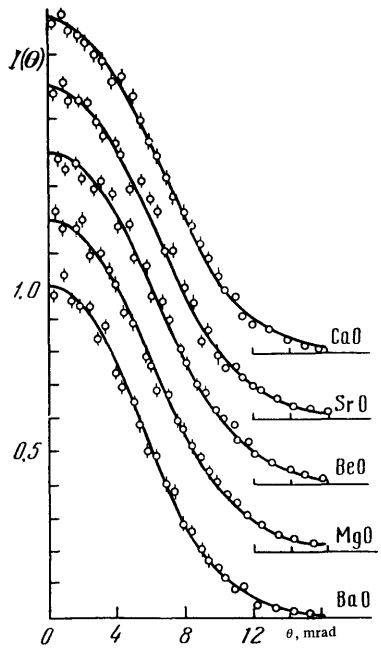


Figure 7. Theoretical (continuous line) and experimental (points) angular correlations for annihilation quanta in alkaline earth metal oxides (BeO and MgO were sintered, the others were in powder form).

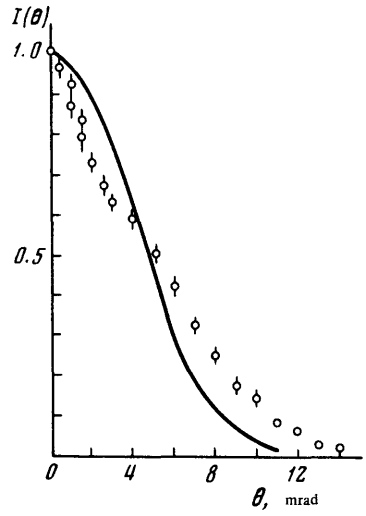


Figure 8. Theoretical (continuous line) and experimental (points) angular correlations for annihilation quanta in zirconium oxide.

We can now proceed directly to the problem of determining the effective charges of atoms from the chief characteristics of the annihilation of positrons in media of the ionic type. The possibility of determining the effective charges of anions from the half-width of correlation curves was first demonstrated for the example of metal oxides[10]. Values have been obtained for the effective charges of F^-, Cl^-, and O^{2-} ions in crystals of various alkali metal halides and quartz from the short lifetimes of positrons with respect to annihilation[37]. It may be noted that in Ref. 10, as in later papers[12,14,16-18], the constants $C^{\Gamma}_{ns,p}$ in Eqn. (7) were given empirical values chosen to give best agreement between the calculated charges and the values of the charges determined by other methods. Thus for example the semi-empirical value of $C^{\Gamma}_{2s,p}$ for the oxides is ~ 3.78,[10] which is slightly greater than the theoretical value $C^{\Gamma}_{2s,p} = 3.52$ (see Table 1). This difference is not so significant, however, if we allow for the accuracy of the determination of the effective charges and the scatter in the results obtained by different methods.

Table 2. Half-width of the correlation curves (~ ±0.2 mrad) and effective charge of the oxygen ion in metal oxides*.

Oxides	Γ, mrad	$\eta, -e$	Oxides	Γ, mrad	$\eta, -e$	Oxides	Γ, mrad	$\eta, -e$
BeO**	13.8	1.33	Sb_2O_3	11.8	0.95	Co_2O_3	13.0	1.18
MgO**	12.8	1.14	Sc_2O_3	12.1	1.01	NiO	12.2	1.03
MgO***	12.1[19]	1.01	TiO_2	12.4	1.07	CuO	12.4	1.07
CaO	14.4	1.45	V_2O_5	11.4	0.88	ZnO	12.2	1.03
SrO	14.2	1.41	Cr_2O_3	14.8	1.52	ZrO_2	12.6	1.10
BaO	12.0	0.99	MnO	13.0	1.18	Nb_2O_5	12.6	1.10
Al_2O_3***	15.3	1.62	Mn_3O_4	13.4	1.26	MoO_3	13.5	1.27
SiO_2***	12.8	1.14	MnO_2	13.0	1.18	La_2O_3	12.8	1.14
SiO_2	11[1]	0.80	FeO**	12.7	1.12	Ce_2O_3	13.4	1.26
GeO_2	11.9	0.97	Fe_3O_4**	13.7	1.31	HfO_2	13.0	1.18
SnO_2	14.4	1.45	Fe_2O_3**	14.3	1.43	Ta_2O_5	12.2	1.03
PbO	12.0	0.99	Co_3O_4	14.0	1.37	WO_3	13.6	1.29

* For the oxides for which the correlation curves have a narrow component, Table 2 gives the half-widths of the broad components;
** sintered;
*** single crystals; the other oxides were taken in the form of powders.

We shall use the theoretical values of the constants $C^{\Gamma}_{ns,p}$ throughout. The effective charges on the anions in various ionic crystals, calculated from the half-widths of the correlation curves (see Eqn. (7) and Table 1), are given in Table 2 (see also Table 5). In those instances where the correlation curves show the presence of a narrow component (for example La_2O_3, TiO_2, GeO_2, ZrO_2, HfO_2, and PbO), the effective charge was determined from the half-width of the broad component. The broad component from the correlation curves can be separated by the "parabola" method, based on the fact that the theoretical $I(\theta)$ curve in the "optical" positron model has the form of a parabola for angles $\theta < 4$ mrad. The narrow component lies in the part of the experimental $I(\theta)$ curve above the parabola (Fig. 9) and the part of the experimental curve remaining after the subtraction of the narrow component is the broad component. When determining the charges of ions from the half-widths of the correlation curves for those compounds in which positronium formation is possible, it should be noted that the best results can be obtained for specimens in the form of single crystals or specimens obtained by sintering powders: in this instance the correlation curves do not have a narrow component[11].

Improved results can also be achieved by carrying out the measurements under vacuum conditions; this produces a marked decrease in the intensity of the narrow component (see, for example, Refs. 11 and 38). The agreement between the effective charge of the oxygen anion, calculated from the half-width of the correlation curves, and the charges found by other methods [39-51]—Szigeti's method, the X-ray spectral method, etc. [52]—is illustrated in Table 3.

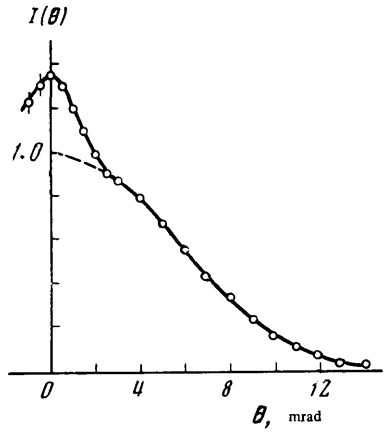


Figure 9. Separation of the broad component from the correlation curve for zirconium oxide by the "parabola" method (the parabola is given by the broken line).

The results in Table 2 lead to various conclusions regarding the magnitude of the effective charge on the oxygen ion in simple metal oxides. The effective charge of the oxygen ion in metal oxides: a) is generally much smaller than its formal value ($-2e$); b) does not change monotonically in the series of alkaline earth metal oxides; c) for the same oxidation state (transition metal oxides), it increases from the start of a period and then decreases towards its end (see, for example, the nickel group), the maximum charge corresponding to the group VI atom (for example the Cr atom); departures from this rule are shown by oxides of the A_3O_4 type (A = Mn, Fe, or Co), for which the charge increases on going from Mn to Co; d) for the same oxidation state (transition metal oxides), in a group of the Mendeleev Table, it increases or remains constant with increase in the atomic number (for example, from Ti to Hf, from V to Ta, and from Mo to W); and e) with increase in the oxidation state, the effective charges of the metal atoms in manganese and iron oxides increase, whereas in cobalt oxides they coincide, within the limits of the formal error in the measurements ($\sim \pm 0.04\ e$) (see Table 4).

Table 4. Effective charge on the metal atom in oxides of manganese, iron, and cobalt.

Manganese oxides (powders)	η, +e	Iron oxides (sintered)	η, +e	Cobalt oxides (powders)	η, +e
MnO	1.18	FeO	1.12	—	—
Mn_3O_4	1.68	Fe_3O_4	1.75	Co_3O_4	1.83
—	—	Fe_2O_3	2.15	Co_2O_3	1.76
MnO_2	2.36	—	—	—	—

Another interesting feature is that the values of the charges on the iron atoms correspond to the fact that the lattice of the oxide Fe_3O_4 contains iron atoms in different oxidation states Fe^{II} and Fe^{III}, in the ratio 1 : 2. The following point must be made regarding conclusion (e): according to results obtained by the X-ray spectral method [47], in compounds of "multivalent" elements the effective charges do not increase, but on the contrary decrease, with increase in the formal valency. A possible reason for this discrepancy is [12] the different physical significance attached to the concept of effective charge in the different methods (see note on p. 229 of Ref. 43).

Table 3. Comparison of the effective charges of the oxygen ion in metal oxides, determined by different methods.

Method and references	Oxides														
	BeO	MgO	CaO	SrO	BaO	Al_2O_3	SiO_2	TiO_2	MnO	FeO	Fe_2O_3	NiO	ZnO	ZrO_2	WO_2
Annihilation of positrons	1.33	1.01 1.14	1.45	1.41	0.99	1.62	0.80 1.14	1.07	1.18	1.12	1.43	1.03	1.03	1.10	1.29
Szigeti's method [39]	—	1.76	1.56	1.16	—	—	—	1.30	—	—	—	—	—	—	—
Ditto [40]	—	1.20	1.56	1.16	—	—	—	—	—	—	—	—	—	—	—
» [41]	1.1	—	—	—	—	—	—	—	—	—	—	—	—	—	—
» [42]	—	1.20	1.18	1.22	—	—	—	—	—	—	—	—	—	—	—
» [43]	—	—	—	—	—	—	—	—	—	—	—	—	1.06	—	—
X-Ray spectral method [44]	—	1.01	—	—	—	1.02	0.98	—	—	—	1.05	—	—	—	—
From heats of sublimation [45]	—	1.08	—	—	—	0.82	0.84	0.80	—	1.03	—	1.00	0.88	0.84	0.56
From heats of formation [46]	—	1.48	1.62	1.60	—	—	—	—	—	—	—	—	1.20	—	—
From interatomic distances [47]	1.18	1.42	1.32	1.40	1.36	—	—	1.02	1.34	1.32	—	1.30	1.24	1.10	—
Theoretical calculation [48]	—	1.56	1.66	1.68	—	—	—	—	—	—	—	—	1.32	—	—
Ditto [49]	—	—	1.46	1.18	0.91	—	—	—	—	—	—	—	1.21	—	—
» [50]	—	1.0 1.1	1.2 1.5	1.2 1.3	1.0 1.1	—	—	—	—	—	—	—	—	—	—
» [51]	1.06	1.20	1.36	1.40	1.44	—	—	—	—	—	—	—	1.08	—	—

As noted above, the effective charges on anions can be determined from the lifetimes of positrons (see Eqn. (8) and Table 1). The effective charges of anions in ionic crystals, determined in this way, agree well with the values found by other methods (Table 5). In the calculation of the charges given in Table 5, the lifetimes of the positrons were given the shortest value, usually denoted by τ_1, except for the bromides and iodides of copper, silver, gold, and thallium, where we used the times τ_2, since for these compounds the values of τ_1 lie much lower than the corresponding $\tau(\eta)$ curves calculated from the "optical" positron model. We used the published values of the lifetimes of the positrons for the alkali metal halides[9], the alkaline earth metal halides[22], copper, silver, gold, and thallium halides[23], crystalline and fused quartz[53], vanadium oxide[26], and nitrides[24]. The half-widths of the correlation curves were determined from published graphs for the alkali metal chlorides and sodium halides[8], LiF,[54] KI, AlN,[19] FeS, and Na_2S.[55]

Table 5. Effective charges of the anions in ionic compounds, determined by the positron-annihilation and other methods.

Ion	Compound	Positron lifetimes*		Angular correlation*		Values of η ($-e$) found by Szigeti's method, the X-ray spectral method, etc.						
						references						
		$10^{-10}\tau$, s	η, $-e$	Γ, mrad	η, $-e$	39	52	40	44	45	47	51
F^-	LiF	1.31±0.07	0.78	12.0	0.65	0.87	0.83	0.80		0.73	0.67	0.76
	NaF	1.93±0.10	0.67	10.5	0.37	0.93	0.94	0.83	0.58	—	—	—
	KF	1.80±0.09	0.69	—	—	—	0.96	0.82	—	—	—	—
	RbF	1.55±0.08	0.73	—	—	—	0.93	—	—	—	—	—
	CsF	1.45±0.08	0.75				0.88	—				
	MgF_2	1.70±0.09	0.70	—	—	—	—	—	—	—	0.68	—
	CaF_2	1.79±0.09	0.69	—	—	0.74	—	—	—	0.69	0.66	—
	SrF_2	1.74±0.09	0.70	—	—	0.65	—	—	—	—	0.69	—
	BaF_2	1.76±0.09	0.70	—	—	0.70	—	—	—	—	0.68	—
Cl^-	LiCl	2.36±0.12	0.72	9.2	0.87	—	0.72	0.67	—	—	—	—
	NaCl	3.13±0.16	0.61	8.6	0.73	0.74	0.74	0.75	0,92	0.79	—	0.64
	KCl	2.75±0.14	0.66	8.3	0.66	0.80	0.79	0.80	—	0.83	—	—
	RbCl	1.99±0.10	0.79	8.6	0.73	0.84	0.87	0.84	—	0.83	—	—
	CsCl	2.02±0.11	0.79	8.9	0.79	0.84	0.87	0.86	—	—	—	—
	$BaCl_2$	2.93±0.15	0.59	—	—	—	—	—	—	—	—	—
	CuCl	1.81±0.09	0.84	—	—	1.10	0.98	1.00	—	—	—	—
	AgCl	1.81±0.09	0.84	—	—	—	0.69	0.71	—	0.77	—	—
	TlCl	1.97±0.10	0.79	—	—	1.08	0.88	1.10	—	0.65	—	—
Br^-	LiBr	2.97±0.15	0.71	—	—	—	0.68	0.74	—	—	—	—
	NaBr	2.92±0.15	0.72	7.4	0.60	0.69	0.71	0.70	0.83	0.77	0.86	0.60
	KBr	3.47±0.17	0.64	—	—	0.76	0.77	0.76	—	—	—	—
	CsBr	3.39±0.17	0.65	—	—	0.79	0.81	0.80	—	—	—	—
	$CaBr_2$	2.62±0.13	0.78	—	—	—	—	—	—	—	—	—
	$SrBr_2$	2.72±0.14	0.76	—	—	—	—	—	—	0.74	—	—
	CuBr	3.81±0.15	0.60	—	—	0.995	0.96	0.86	—	—	0.63	—
	AgBr	3.47±0.15	0.64	—	—	—	0.66	0.67	—	—	0.73	—
	TlBr	3.65±0.15	0.62	—	—	—	0.84	1.06	—	—	—	—
I^-	LiI	3.27±0.17	~1	—	—	—	0.55	0.50	—	—	—	—
	NaI	3.28±0.18	~1	6.8	0.62	0.71	0.70	0.71	0.75	—	—	0.54
	KI	4.01±0.20	0.72	7.1	0.71	0.69	0 70	0.73	—	0.79	0.80	—
	RbI	4.25±0.21	0.68	—	—	0.89	0.81	—	—	—	—	—
	CsI	3.55±0.20	0.86	—	—	—	0.74	—	—	—	—	—
	SrI_2	3.87±0.19	0.75	—	—	—	—	—	—	—	—	—
	CuI	3.79±0.15	0.77	—	—	—	0.91	—	—	—	0.60	—
	AgI	3.70±0.15	0.80	8.5	1.08	—	0.70	—	—	0.79	0.72	—
	AuI	3.86±0.20	0.75	—	—	—	—	—	—	—	—	—
	TlI	3.76±0.15	0.78	—	—	—	0.83	—	—	—	—	—
O^{2-}	SiO_2 (cryst.)	2.0±0.33	0.68	—	—	—	—	—	0.98	0.65	—	—
	SiO_2 (fused)	3.5±0.5	0.56	—	—	—	—	—		—	—	—
	V_2O_3	1.94±0.13	0.69									
S^{2-}	Na_2S	—	—	8,3	0.91	—	—	—	0.96	—	—	—
	FeS	—	—	10.3	1.38	—	—	—	0.71—0,96	—	—	—
N^{3-}	BN	2.64±0.08	0.66	—	—	—	—	—	—	—	1.62	0.76
	AlN	2.90±0.10	0.63	11.1	1.15	—	—	—	1.32	—	—	1.20

* The references to the papers from which the values of τ and Γ were taken are given in the text.

The data given in Tables 2 and 5 (see also below) confirm again the view, recently developed by Syrkin and his school[56,57], that inorganic compounds do not contain multiply-charged anions; the charges of anions in compounds are generally much smaller than their formal values.

Table 6. Comparison of the half-widths of the correlation curves, the effective charge of the oxygen ion, and the melting points of molybdates and tungstates.

Molybdates	Γ, mrad	η, $-e$	M.p., °C	Tungstates	Γ, mrad	η, $-e$	M.p., °C
Li_2MoO_4	12.4	1.07	705	Li_2WO_4	10.8	0.77	738
Na_2MoO_4	13.1	1.20	688	Na_2WO_4	12.9	1.16	698
K_2MoO_4	12.3	1.05	926	K_2WO_4	11.3	0.86	926
Rb_2MoO_4	12.4	1.07	929	Rb_2WO_4	11.2	0.84	959
Cs_2MoO_4	12.2	1.03	925	Cs_2WO_4	11.1	0.82	958
$LiSc(MoO_4)_2$	12.8	1.14	820	$LiSc(WO_4)_2$	11.4	0.88	975
$NaSc(MoO_4)_2$	13.5	1.27	920	$NaSc(WO_4)_2$	13.2	1.22	820
$KSc(MoO_4)_2$	12.9	1.16	1100	$KSc(WO_4)_2$	12.2	1.03	1120
$RbSc(MoO_4)_2$	12.3	1.05	1110	$RbSc(WO_4)_2$	11.7	0.93	1190
$CsSc(MoO_4)_2$	11.6	0.91	1120	$CsSc(WO_4)_2$	11.3	0.86	1250
$Sc_2(MoO_4)_3$	12.4	1.07	—	$Sc_2(WO_4)_3$	12.2	1.03	—

The positron method can be used to determine effective charges not only in binary inorganic compounds, but also in more complex compounds, for example in mixed metal oxides[17] and in multi-component inorganic glasses[13,16]. The possibility of using the "optical" positron model to determine the charges of anions in glasses is based on the fact that this model does not assume the existence of long-range order. In complex compounds, when the anion can occupy several non-equivalent positions in the lattice, the charge found for the anion will represent a value averaged over these positions. As an example of the determination of the effective charge of anions in complex compounds, Table 6 gives the charges of the oxygen ion in molybdates and tungstates, calculated from the half-widths of the correlation curves (see Eqn. (7) and Table 1). The correlation curves for these compounds, with the exception of lithium tungstate (Li_2WO_4), do not contain a narrow component. A noteworthy feature is the correlation between the change in the magnitude of the charge on the oxygen ion and the melting points of the alkali metal molybdates and tungstates and the double molybdates and tungstates of the alkali metals and scandium (in each of the four groups of compound, they change in opposite fashion in the series of atoms Li–Cs): the maximum charge corresponds to the minimum melting point in the compounds containing sodium atoms. It would appear that the compound $NaSc(MoO_4)_2$ does not obey this rule, but the study of the structure of this compound shows a polymorphic transformation at 600°. It may therefore be stated that the "melting point" of the low-temperature modification of $NaSc(MoO_4)_2$ must be lower than the melting point of the $LiSc(MoO_4)_2$ crystal. The above correlation between the relative change in the effective charge on the anion and the melting point is apparently a general characteristic of analogous compounds containing alkali metal atoms. An example confirming this conclusion is provided by the alkali metal fluorides and chlorides[17]. In this instance, in contrast to the situation for the molybdates and tungstates, the maximum melting point corresponds to the sodium halides.

Interesting results were obtained in the study of the behaviour of the effective charge on anions in the crystal–glass transition[13,16,18]. Table 7 gives the half-widths of the correlation curves and the effective charges of the oxygen ion for a number of three-component glasses, where, in contrast to the situation for one- and two-component glasses, positronium formation is not detected from the results of measurements of the angular correlation and the lifetimes of the positrons. Comparison of the values of the charges on the oxygen ion in corresponding crystalline oxides (Table 2) and glasses (Table 7) shows that the effective charge on the oxygen ion decreases systematically in the crystal–glass transition§. This conclusion is also confirmed[18] for binary compounds of the (IV–V) and (IV–VI) type. Thus the change to the vitreous state is accompanied by a redistribution of the valency electrons which increases the proportion of the covalent component in the chemical bonds.

Table 7. Half-widths of the correlation curves and effective charge on the oxygen ion in various oxygen-containing glasses.

Composition of glass, mole %	Γ, mrad	η, $-e$
76.2 SiO_2·19.0 Li_2O·4.8 SnO_2	10.6	0.72
76.2 SiO_2·19.0 Na_2O·4.8 SnO_2	11.2	0.84
76.2 SiO_2·19.0 K_2O·4.8 SnO_2	11.6	0.91
84.3 B_2O_3·13.7 Na_2O·2.0 Fe_2O_3	12.0	0.99
76.2 B_2O_3·19.0 Na_2O·4.8 SnO_2	11.8	0.91
63.5 CaO·31.7 Al_2O_3·4.8 SnO_2	11.5	0.89

In tin-containing glasses with the equimolar composition, an increase in the effective charge of the oxygen ion is observed when one alkali metal ion is replaced by another in the order Li–K (see Table 7). In this instance the change in the charge on the oxygen ion is confirmed[13] by measurements of the chemical shift of the Mössbauer absorption line; the chemical shift in glasses with the composition indicated is negative relative to crystalline tin(IV) oxide, and its absolute value increases on going from Li to K, indicating[58] an increase in the ionic character of the Sn–O bonds in this order. In alkali silicate glasses with the equimolar composition, as in mixed metal oxides, a correlation is observed between the change in the effective charge and various macroscopic properties. Thus the increased magnitude of the charge on the oxygen ion on going from the lithium silicate glass to the potassium silicate glass corresponds to an increase, in the same sense, in the coefficient of thermal expansion and a decrease in the micro-hardness of the glass.

Determination of the effective charge on the oxygen atom in water (the half-width of the broad component of the correlation curve is approximately 10 mrad[59]) gives the value $-0.6\,e$, which is almost twice the calculated value of $-0.26\,e$[60]; this is possibly due to the approximate nature of the "optical" positron model for the description of the characteristics of annihilation positrons in water.

§ The "positron" effective charge of the oxygen ion in alkali metal oxides is not known, but the value calculated from the heats of sublimation for Na_2O is $-1.10\,e$.[45]

The "optical" positron model cannot be used to determine the charge of the H^- ion in metal hydrides, since in the hydrides the positron is apparently present simultaneously in the field of several H^- ions; this is indicated by the dependence of the lifetimes of the positrons on the density of the hydrides[61]. A more rigorous calculation of the characteristics of the annihilation, with allowance for the distribution of electron density in the LiH molecule by the MO method, carried out[62] for the LiH crystal, gives the value $-0.60\,e$ for the charge of the H^- ion, this is fairly close to the published value of $-0.52\,e$.[63] Thus the above results indicate that the positron-annihilation method can be regarded as a new *independent* method for determining the effective charges of the anions in compounds of the ionic type.

In conclusion it may be noted that the determination of the charges of anions is not the only possible application of the positron-annihilation method in the chemistry of ionic compounds. Recent results[25,64–67] show that the annihilation characteristics of positronium atoms, for example in highly dispersed oxide powders, depend markedly on the physicochemical properties of their surfaces and the filling of the pores. It can already be stated that further studies in this direction will make it possible to use the positron-annihilation method to study adsorption phenomena.

REFERENCES

1. G. S. Zhdanov (Editor), in collected papers "Annigilatsiya Pozitronov v Tverdykh Telakh" (Collected Papers on the Annihilation of Positrons in Solids), Inostr. Lit., Moscow, 1960.
2. "Positron Annihilation" (Proc. Conf. Positron Annihilation, Wayne State Univ., Detroit, Mich. USA July 26–30, 1965. Edited by A. T. Stewart and L. O. Roellig, Academic Press, New York–London, 1967).
3. V. I. Gol'danskii, "Fizicheskaya Khimiya Pozitronov i Pozitroniya" (The Physical Chemistry of Positrons and Positronium), Izd. Nauka, Moscow, 1968.
4. I. Ya. Dekhtyar, Czech. J. Phys., 188, 1509 (1968).
5. V. L. Sedov, Uspekhi Fiz. Nauk, 94, 417 (1968).
6. V. I. Gol'danskii and E. P. Prokop'ev, Fiz. Tverd. Tela, 8, 515 (1966).
7. A. T. Stewart, Canad. J. Phys., 35, 168 (1957).
8. A. T. Stewart and N. K. Pope, Phys. Rev., 120, 2033 (1960).
9. C. Bussolati, A. Dupasquier, and L. Zappa, Nuovo Cimento, 52B, 529 (1967).
10. A. D. Tsyganov, A. Z. Varisov, A. D. Mokrushin, and E. P. Prokop'ev, Fiz. Tverd. Tela, 11, 2079 (1969).
11. G. M. Bartenev, A. Z. Varisov, V. I. Gol'danskii, B. M. Levin, A. D. Mokrushin, and A. D. Tsyganov, Fiz. Tverd. Tela, 11, 3177 (1969).
12. G. M. Bartenev, A. D. Tsyganov, and A. Z. Varisov, Fiz. Tverd. Tela, 12, 669 (1970).
13. G. M. Bartenev, S. M. Brekhovskikh, A. Z. Varisov, L. M. Landa, and A. D. Tsyganov, Fiz. Tverd. Tela, 12, 1249 (1970).
14. G. M. Bartenev, A. Z. Varisov, V. I. Gol'danskii, and A. D. Tsyganov, Zh. Strukt. Khim., 11, 287 (1970).
15. G. M. Bartenev, A. D. Tsyganov, A. Z. Varisov, and E. P. Prokop'ev, Zhur. Eksper. Teor. Fiz., 58, 1904 (1970).
16. G. M. Bartenev, S. M. Brekhovskikh, A. Z. Varisov, L. M. Landa, and A. D. Tsyganov, Izv. Akad. Nauk SSSR, Neorg. Materialy, 6, 1553 (1970).

17. G. M. Bartenev, V. A. Balashov, A. Z. Varisov, A. A. Maier, and A. D. Tsyganov, Izv. Akad. Nauk SSSR, Neorg. Materialy, No. 1 (1971).
18. A. D. Tsyganov, S. A. Dembovskii, and V. I. Mikhailov, Fiz. i Tekhn. Poluprovodnikov, 11, 2184 (1970).
19. A. S. Klotz and D. W. Hafemeister, J. Chem. Phys., 49, 5326 (1968).
20. F. Badoux, F. Heinrich, and G. Kallmeyer, Helv. Phys. acta, 40, 375 (1967).
21. W. Brandt, G. Coussot, and R. Paulin, Phys. Rev. Letters, 23, 522 (1969).
22. G. Gambarini and L. Zappa, Phys. Rev. Letters, 27A, 498 (1968).
23. S. Cova, A. Dupasquier, and M. Manfredi, Nuovo Cimento, 47B, 263 (1967).
24. A. Gainotti and C. Ghezzi, Lett. Nuovo Cimento, 2, 734 (1969).
25. P. Sen and A. P. Patro, Nuovo Cimento, 64B, 324 (1969).
26. A. Gainotti, C. Ghezzi, and M. Manfredi, Nuovo Cimento, 62B, 121 (1969).
27. E. P. Prokop'ev, Candidate's Thesis, Institute of Chemical Physics, Academy of Sciences of the USSR, Moscow, 1965.
28. G. M. Bartenev, A. D. Tsyganov, E. P. Prokop'ev, and A. Z. Varisov, Izv. Vys. Ucheb. Zaved., Fizika, No. 4, 68 (1971).
29. J. W. Shearer and M. Deutsch, Phys. Rev., 82, 336 (1951).
30. S. A. Colgate, F. C. Gilbert, and S. Violett, Phys. Rev., 88, 1435 (1952).
31. H. W. Kendall and M. Deutsch, Phys. Rev., 93, 932 (1954).
32. J. B. Gerhart, B. C. Carlson, and R. Sherr, Phys. Rev., 94, 917 (1954).
33. V. I. Gol'danskii, A. V. Ivanova, and E. P. Prokop'ev, in collected papers "Yadernaya Khimiya" (Collected Papers on Nuclear Chemistry), Izd. Nauka, Moscow, 1965, p. 249.
34. Chang Li, Vestnik Leningrad. Gos. Univ., Ser. Fiz. Khim., No. 4, 160 (1958).
35. A. A. Tkachenko, Vestnik Leningrad. Gos. Univ., Ser. Fiz. Khim., No. 22, 167 (1958).
36. V. I. Gol'danskii, A. V. Ivanova, and E. P. Prokop'ev, Zhur. Eksper. Teor. Fiz., 47, 659 (1964).
37. V. I. Gol'danskii, E. P. Prokop'ev, and A. D. Tsyganov, Zhur. Strukt. Khim., 11, 1123 (1970).
38. J. H. Kusmiss and A. T. Stewart in Ref. 2, p. 341.
39. B. Szigeti, Trans. Faraday Soc., 45, 155 (1949).
40. K. B. Tolpygo, in collected papers "Khimicheskaya Svyaz' v Poluprovodnikakh i Tverdykh Telakh" (Collected Papers on Chemical Bonding in Semiconductors and Solids), Minsk, 1965, p. 152.
41. E. Loh, Phys. Rev., 166, 672 (1968).
42. J. L. Jacobsen and E. R. Nixon, J. Phys. Chem. Solids, 29, 967 (1968).
43. R. J. Collins and D. A. Kleinman, J. Phys. Chem. Solids, 11, 190 (1959).
44. R. L. Barinskii and V. I. Nefedov, "Rentgenospektral'noe Opredelenie Zaryada Atomov v Molekulakh" (The X-ray Spectral Determination of the Charges of Atoms in Molecules), Izd. Nauka, Moscow, 1966.
45. V. S. Urusov, Zhur. Strukt. Khim., 7, 439 (1966).
46. H. Gutbier, Naturforsch., 19a, 1154 (1964).
47. E. S. Sarkisov, Izv. Akad. Nauk SSSR, Neorg. Materialy, 5, 441 (1969).
48. H. Kimmel, Naturforsch., 20a, 359 (1965).
49. J. P. Suchet, "Chimie Physique de Semiconducteurs" (Translated into Russian), Izd. Metallurgiya, Moscow, 1964.
50. A. A. Levin, Ya. K. Syrkin, and M. E. Dyatkina, Zhur. Strukt. Khim., 7, 757 (1966).
51. B. V. Nekrasov, Dokl. Akad. Nauk SSSR, 187, 338 (1969).
52. E. V. Dulepov and S. S. Batsanov, Zhur. Strukt. Khim., 10, 154 (1969).
53. R. E. Bell and R. E. Graham, Phys. Rev., 90, 644 (1953).
54. G. Lang and S. DeBenedetti, Phys. Rev., 108, 914 (1957).
55. P. Colombino, I. Degregori, L. Mayrone, L. Trossi, and S. DeBenedetti, Phys. Rev., 119, 1665 (1960).
56. Ya. K. Syrkin, Uspekhi Khim., 31, 397 (1962) [Russ. Chem. Rev., No. 4 (1962)].
57. A. A. Levin, Ya. K. Syrkin, and M. E. Dyatkina, Uspekhi Khim., 38, 193 (1969) [Russ. Chem. Rev., No. 2 (1969)].
58. V. I. Gol'danskii, "Effekt Messbauera i ego Primenenie v Khimii" (The Mössbauer Effect and Its Applications in Chemistry), Izd. Akad. Nauk SSSR, Moscow, 1963.
59. P. Colombino, B. Fiscella, and L. Trossi, Nuovo Cimento, 38, 707 (1965).
60. J. L. Rosenfeld, J. Chem. Phys., 40, 384 (1964).
61. A. Gainotti, C. Ghezzi, M. Manfredi, and L. Zecchina, Nuovo Cimento, 56B, 47 (1968).
62. W. Brandt, L. Eder, and S. Lundqvist, Phys. Rev., 142, 165 (1966).
63. R. S. Calder, W. Cochran, D. Griffiths, and R. D. Lowde, J. Phys. Chem. Solids, 23, 621 (1962).
64. A. D. Tsyganov, A. L. Mokrushin, and E. P. Prokop'ev, Kinetika i Kataliz, 11, 808 (1970).
65. V. I. Gol'danskii, B. M. Levin, A. D. Mokrushin, M. A. Kaliko, and M. N. Pervushina, Dokl. Akad. Nauk SSSR, 191, 855 (1970).
66. G. M. Bartenev, A. Z. Varisov, V. I. Gol'danskii, M. N. Pletnev, E. P. Prokop'ev, and A. D. Tsyganov, Dokl. Akad. Nauk SSSR, 197, 560 (1971).
67. S. Y. Chuang and S. J. Tao, J. Chem. Phys., 52, 749 (1970).

Department of Solid State Physics,
Lenin Moscow State Pedagogic
Institute